

# Low Dielectric Constant Materials for High Performance LCDs

Haiwei Chen,<sup>1</sup> Fenglin Peng,<sup>1</sup> Shin-Tson Wu,<sup>1</sup> Minggang Hu,<sup>2</sup> Jian Li,<sup>2</sup> Zhongwei An,<sup>2</sup>  
Ming-Chun Li,<sup>3</sup> Seok-Lyul Lee,<sup>3</sup> and Weng-Ching Tsai<sup>3</sup>

<sup>1</sup>College of Optics and Photonics, University of Central Florida, Orlando, Florida 32816, USA

<sup>2</sup>Xi'an Modern Chemistry Research Institute, 168 Zhangba Rd. East, Xi'an, China

<sup>3</sup>AU Optronics Corp., Hsinchu Science Park, Hsinchu 300, Taiwan

## Abstract

A small  $|\Delta\epsilon|$  LC mixture exhibits an ultra-low viscosity, low activation energy, and high transmittance yet at a reasonably low voltage. Its response time remains 42 ms even at  $-20^\circ\text{C}$ . These materials are attractive for fringing field switching-based mobile displays, IPS-based 4K2K TVs, and MTN-based wearable LCoS projection displays.

## Keywords

Fringe field switching (FFS); Liquid crystal displays (LCDs).

## 1. Introduction

Mobile displays and wearable displays are growing rapidly [1]. These displays are often used outdoors and have to endure severe weather conditions, like low temperatures ( $-20^\circ\text{C}$ ). In such ambient condition, the response time is usually as slow as hundreds of milliseconds. Slow response time causes motion image blur and crosstalk, which in turn leads to degraded color saturation.

To overcome the above mentioned problems, in this paper, we find that fringe field switching (FFS) with a low dielectric constant LC can offer an excellent solution. Such a small  $\Delta\epsilon$  LC based LCD exhibits several outstanding features: high transmittance, fast response time (even at  $-20^\circ\text{C}$ ), suppressed flexoelectric effect for p-FFS, and the inherent advantages like wide view, weak color shift, and pressure resistance for touch panels [2,3]. Therefore, it is a strong contender for next-generation LCDs, especially for mobile devices, wearable displays and car navigators.

## 2. Results and Discussion

### 2.1 Fringe Field Switching with Positive $\Delta\epsilon$ LC (p-FFS)

In experiment, we compared its electro-optic properties of a small  $\Delta\epsilon$  LC mixture called MCRI-23204 (Xi'an Modern Chemistry Research Institute, China) with Merck MLC-6686. Table 1 lists the physical properties of these two mixtures. MLC-6686 has a relatively large dielectric anisotropy ( $\Delta\epsilon=10$ ) so that its operation voltage is low. However, it has two shortcomings: higher viscosity (because more polar groups are involved) and lower transmittance (because LC directors tend to follow the nonuniform fringing fields).

**Table 1.** Physical properties of two LC mixtures studied ( $T=23^\circ\text{C}$ ,  $\lambda=633\text{nm}$  and  $f=1\text{ kHz}$ )

LC	$\Delta n$	$\epsilon_{  }$	$\epsilon_{\perp}$	$\Delta\epsilon$	$\gamma_1$ (mPa·s)	$K_{22}$ (pN)	$T_c$ ( $^\circ\text{C}$ )
MLC-6686	0.093	14.5	4.5	10.0	102	6.7	71
MCRI-23204	0.100	6.3	2.8	3.5	45	6.0	78

### 2.1.1 Temperature dependent birefringence

We measured the temperature dependent  $\Delta n$  of MCRI-23204 and MLC-6686 at  $\lambda=633\text{ nm}$  using a commercial homogeneous cell with  $d=8\mu\text{m}$ . Results are shown in Fig. 1, where dots stand for measured data and red line for the fitting results using Haller's semi-empirical equation [4, 5]:

$$\Delta n(T) = \Delta n_0 S = \Delta n_0 (1 - T/T_c)^\beta, \quad (1)$$

where  $\Delta n_0$  is the extrapolated birefringence at  $T=0$ ,  $S$  is the order parameter,  $T$  is the temperature,  $T_c$  is the clearing point, and  $\beta$  is the material parameter.

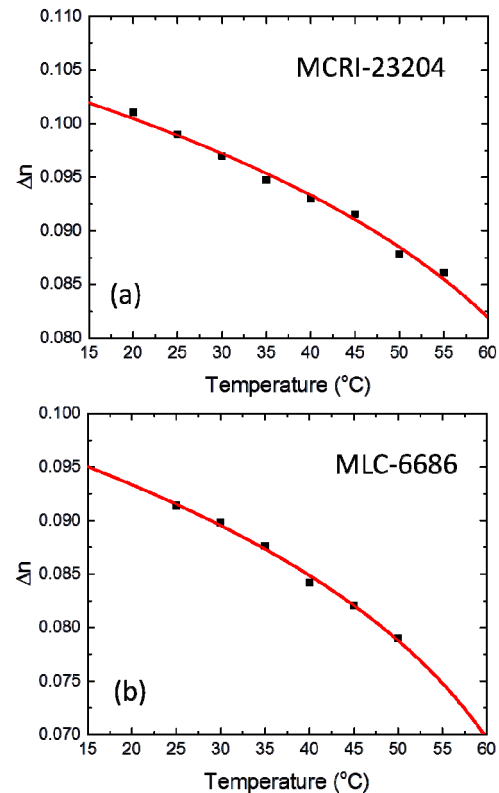


**Fig. 1.** Temperature dependent  $\Delta n$  of (a) MCRI-23204 and (b) MLC-6686 at  $\lambda = 633\text{nm}$ . Dots are experimental data and red lines are fitting curves with Eq. (1).

### 2.1.2 Temperature dependent visco-elastic constant

In a FFS cell, the electric field is not uniform. Thus, it is not easy to derive the analytical expression for the LC response time because both  $K_{11}$  and  $K_{22}$  are involved, although  $K_{22}$  dominates.

Therefore, we measured the response time of MCRI-23204 and MLC-6686 using FFS cells with photoalignment, cell gap  $d=3.5\mu\text{m}$ , electrode width  $w=3\mu\text{m}$ , electrode gap  $l=4\mu\text{m}$ , and rubbing angle  $\varphi=7^\circ$ . Fig. 2(a) shows the measured data.

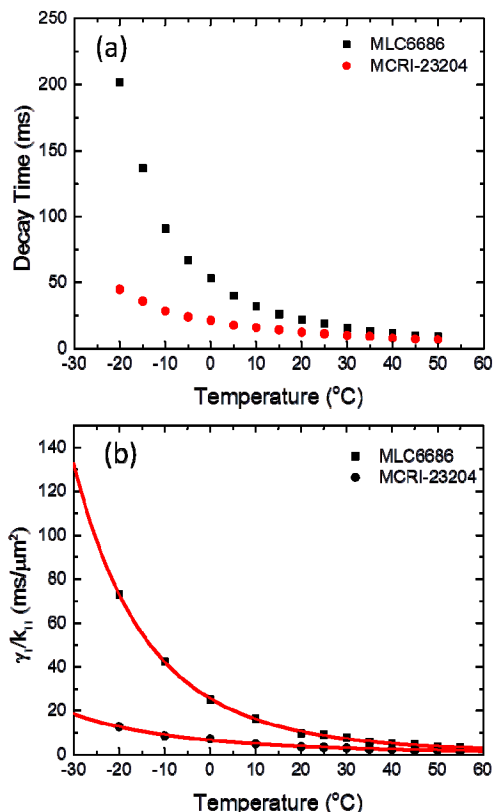


**Fig. 2.** Measured temperature dependent (a) decay time and (b)  $\gamma_1/K_{11}$  of MCRI-23204 and MLC-6686.

From Fig. 2(a), the response time of both materials increases as the temperature decreases, but at different rates. For example, at  $T=25^\circ\text{C}$  the decay time of MLC-6686 is only 2X slower than that of MCRI-23204, but this ratio jumps to 4.5 at  $-20^\circ\text{C}$ . The slower response time at lower temperature is easy to understand because the rotational viscosity increases exponentially as [6]:

$$\gamma_1 \sim S \cdot \exp(E/k_B T), \quad (2)$$

where  $E$  is the activation energy and  $k_B$  is the Boltzmann constant. From Eq. (2), activation energy plays a key role affecting the rising rate of rotational viscosity in the low temperature region. Key parameters affecting activation energy include molecular structure and conformation, and intermolecular interactions [8]. A low  $\Delta\varepsilon$  LC mixture mainly consists of weakly polar and non-polar compounds. As a result, its activation energy is relatively small, which in turn causes a mild increase as the temperature decreases. To validate this hypothesis, we measured the visco-elastic coefficient of MCRI-23204 and MLC-6686 using commercial homogeneous cells with  $d=8\mu\text{m}$ . In theory, temperature dependent visco-elastic constant ( $\gamma_1/K_{ii}$ ) can be described as follows [6-8]:

$$K_{ii} \sim S^2, \quad (3)$$

$$\gamma_1/K_{ii} \sim \exp(E/k_B T)/S, \quad (4)$$

where  $K_{ii}$  is the corresponding elastic constant. Figures 2(b)

depicts the measured  $\gamma_1/K_{11}$  and fitted curves for MCRI-23204 and MLC-6686, respectively. The activation energy we obtained through fitting is  $E=205\text{ meV}$  for MCRI-23204, which is much smaller than that of MLC-6686 ( $E=327\text{ meV}$ ). Because MCRI-23204 has small activation energy, its response time is much less sensitive to the temperature change, as Fig. 2(a) depicts.

### 2.1.3 Voltage-Transmittance curves

To optimize the device performance, we simulate the electro-optic properties of p-FFS cell employing both materials (MCRI-23204 and MLC-6686) with a commercial LCD simulator TechWiz.3D and the extended  $2 \times 2$  Jones matrix method [9]. In order to achieve high transmittance and low operation voltage, we set  $d\Delta n \sim 340\text{nm}$ . To make a fair comparison, we use the same cell parameters during simulations: electrode width  $w=2.5\mu\text{m}$ , electrode gap  $l=3.5\mu\text{m}$ , pretilt angle  $\theta_p=2^\circ$  and rubbing angle  $\varphi=7^\circ$ . Figure 3(a) depicts the simulated VT curves. MCRI-23204 has a smaller  $\Delta\varepsilon$  so that its operation voltage is higher than that of MLC-6686 (5.8V vs. 4.3V) [10]. However, its peak transmittance is 6% higher than that of MLC-6686. Therefore, if we are willing to sacrifice 6% in transmittance, then we can drive the p-FFS cell at 4.5V and obtain the same transmittance ( $\sim 83\%$ ) as MLC-6686.

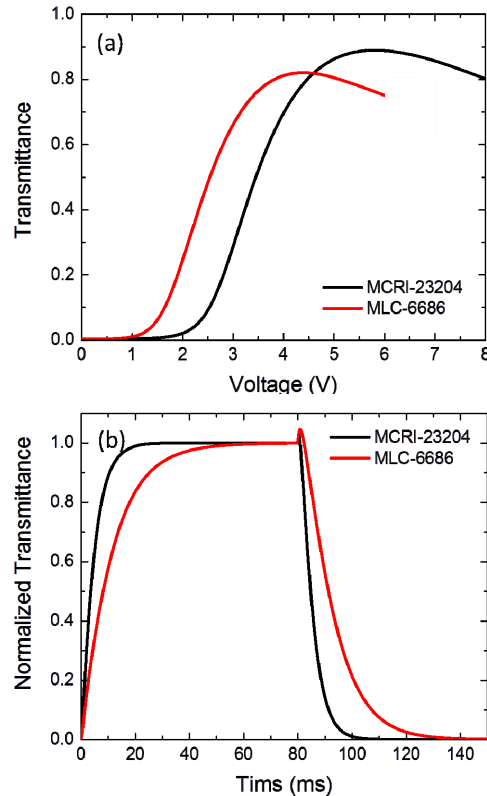


**Fig. 3.** Simulated (a) VT curves and (b) response time of MLC-6686 and MCRI-23204.  $\lambda=550\text{ nm}$ . FFS:  $w=2.5\mu\text{m}$ , and  $l=3.5\mu\text{m}$ .

### 2.1.4 Response time

Another major advantage of such a small  $\varepsilon$  LC material is its ultra-low viscosity [11]. From Table 1, the rotational viscosity of MCRI-23204 is only 45 mPa·s, which is much smaller than that of MLC-6686 (102 mPa·s). We calculated the turn-on and turn-off times from the time-dependent transmittance curves shown in Fig. 3(b). As usual, the response time is defined as

### 31.2 / H. Chen

10%–90% transmittance change. For MLC-6686, the simulated response time [rise, decay] is [23.8ms, 23.4ms], whereas the response time of MCRI-23204 is [10.2ms, 10.6ms]. The ~2.2X faster response time of MCRI-23204 mainly originates from its lower viscosity.

For outdoor applications of LCD devices, the slow response time at low temperature causes severe image blurs and reduced color gamut [12]. From Eq. (2), the rotational viscosity increases exponentially as the temperature decreases. However, MCRI-23204 has a small activation energy ( $E \sim 205$  meV) so that its rotational viscosity in the low temperature region remains relatively low. From Fig. 2, the measured decay time at  $-20^\circ\text{C}$  is 42 ms for the  $3.5\text{-}\mu\text{m}$  cell gap employed. This is still relatively fast at such a low temperature. As reported in [12], the rise time (from 0 to 32nd grayscale without overdrive) of a MVA at  $-20^\circ\text{C}$  is as sluggish as 1000 ms.

#### 2.1.5 Flexoelectric effect

Because of the non-uniform electric field, the splay deformation would occur in p-FFS and electric polarization is induced, which is known as flexoelectric effect [13]. For the low  $\Delta\epsilon$  material, the tilt angle is less sensitive to the electric field, which in turn results in weaker splay deformation [Fig. 4(a)]. But for a large  $\Delta\epsilon$  LC (e.g. MLC-6686), LC directors near the middle of electrodes and gaps tilt at a large angle [Fig. 4(b)]. Therefore, low  $\Delta\epsilon$  material has an extra built-in advantage, which is smaller flexoelectric effect.

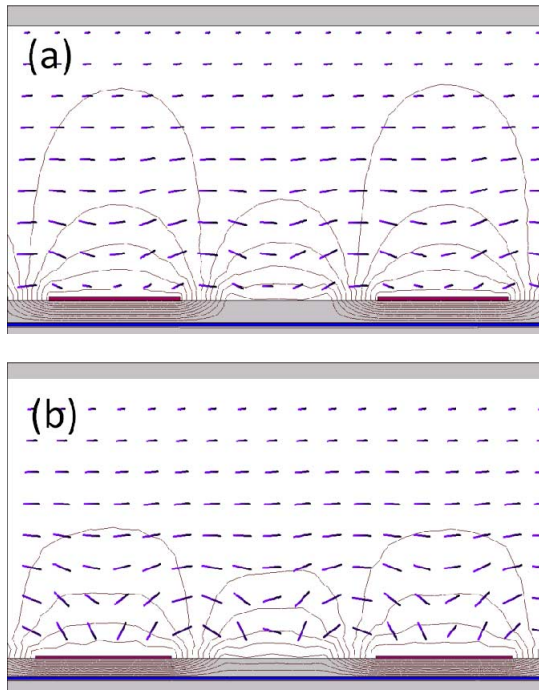


**Fig. 4.** LC director deformation of p-FFS cells with (a) MCRI-23204 and (b) MLC-6686.

#### 2.2 Fringe Field Switching with Negative $\Delta\epsilon$ LC (n-FFS)

For mobile displays, n-FFS is superior to p-FFS in transmittance, but its voltage could be higher depending on the employed  $\Delta\epsilon$  [14]. To lower the operation voltage, a relatively large  $|\Delta\epsilon|$  LC material is developed, like ZOC-7003 [15], whose  $\Delta\epsilon$  is  $-4.4$ . The detailed properties of ZOC-7003 are listed in Table 2.

**Table 2.** Physical properties of ZOC-7003 (JNC, Japan) at  $T=23^\circ\text{C}$ ,  $\lambda=633\text{nm}$ , and  $f=1$  kHz.

LC	$\Delta n$	$\epsilon_{  }$	$\epsilon_{\perp}$	$\Delta\epsilon$	$\gamma_1$ (mPa·s)	$K_{22}$ (pN)	$T_c$ ( $^\circ\text{C}$ )
ZOC-7003	0.101	3.6	8.0	-4.4	101	7.0	79

As  $\Delta\epsilon$  increases, rotational viscosity increases almost linearly. We measured the temperature dependent visco-elastic constant of ZOC-7003 and results are shown in Fig. 5(a). Through fitting, we obtained  $E=396$  meV. Meanwhile, we measured the response time of ZOC-7003 at different temperatures and results are plotted in Fig. 5(b).

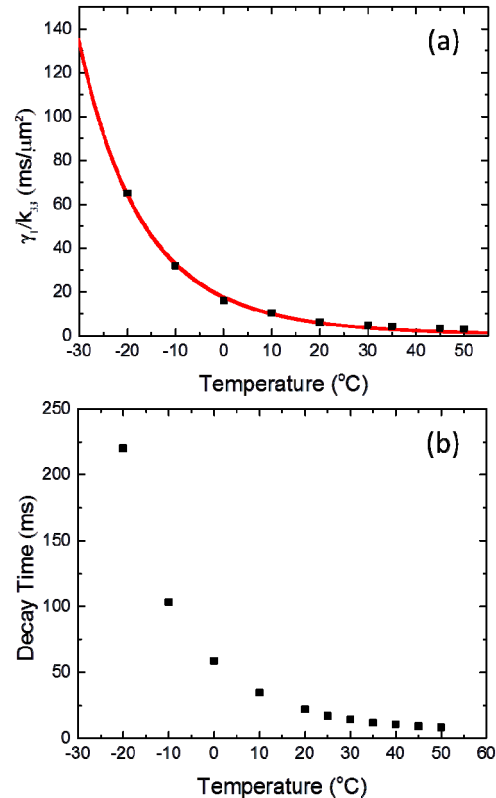


**Fig. 5.** (a) Temperature dependent  $\gamma_1/K_{33}$  and (b) measured decay time of ZOC-7003 using an n-FFS cell.

From Fig. 5(b), the decay time of ZOC-7003 at  $20^\circ\text{C}$  is about 22 ms, but it climbs to 220 ms at  $-20^\circ\text{C}$  because of its relatively large activation energy. This is a big concern for outdoor applications. Using the same strategy as p-FFS mode, we investigated the effect of low  $\epsilon$  materials for n-FFS. Fig. 6 depicts the VT curves of three low  $\Delta\epsilon$  LCs. Unlike p-FFS, the voltage of n-FFS keeps increasing from 4.8V to 6.9V, but no gain in transmittance is observed. This is because the LC orientation is n-FFS cell is already relatively uniform. If the operation voltage is chosen at 5V, then the transmittance of LC mixture with  $\Delta\epsilon=-3$  is only 1% lower than that of ZOC-7003. Even if we fix the voltage at 4.5V, the transmittance is only 4% lower. But the gain in lower viscosity and activation energy would be still significant. The estimated response time is still 2x to 3x faster in the low temperature region. Moreover, faster rise time helps increase transmittance and faster decay time helps reduces cross-talks.

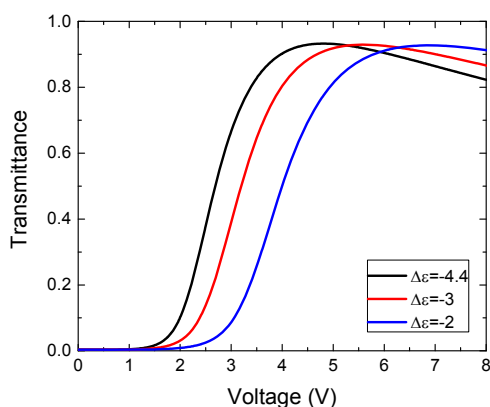


**Fig. 6.** Simulated VT curves of negative  $\Delta\epsilon$  LC materials with different dielectric constants. n-FFS cell:  $w=2.5\mu\text{m}$ ,  $l=3.5\mu\text{m}$ , and  $d\Delta n=320\text{nm}$  at  $\lambda=550\text{nm}$ .

### 3. Conclusion

We have investigated the electro-optic performance of p-FFS and n-FFS LCDs using low  $\Delta\epsilon$  LC materials. Such a low  $\epsilon$  LC material exhibits several attractive properties: ultra-low viscosity and small activation energy, high transmittance, and weak flexoelectric effect for p-FFS mode. The small activation energy (200 meV) keeps the response time relatively fast even at  $-20^\circ\text{C}$ . This is particularly desirable for the outdoor application of mobile or wearable displays. A major concern of the low  $\epsilon$  LC material is its potentially high operation voltage. However, the operation voltage is inversely proportional to the square-root of  $\Delta\epsilon$ . Moreover, this disadvantage can be mitigated by its high transmittance. As a result, we can still obtain high transmittance at a relatively low voltage, while harvesting the fast response time. Using the same strategy discussed above, the proposed low  $\Delta\epsilon$  LC materials could be used in other LC modes, e.g. IPS, TN, mixed-mode twisted nematic (MTN), etc. Fast response time is important for improving transmittance, reducing motion image blurs, and reducing image crosstalk. Therefore, the proposed low  $\Delta\epsilon$  LCs are expected to have widespread applications.

### 4. References

- [1] Y. Takubo, Y. Hisatake, T. Iizuka, and T. Kawamura, "Ultra-high resolution mobile displays," *SID Symp. Dig.* **64**, 869-872 (2012).
- [2] S. H. Lee, S. L. Lee, and H. Y. Kim, "Electro-optic characteristics and switching principle of a nematic liquid crystal cell controlled by fringe-field switching," *Appl. Phys. Lett.* **73**, 2881-2883 (1998).
- [3] S. H. Lee, H. Y. Kim, S. M. Lee, S. H. Hong, J. M. Kim, J. W. Koh, J. Y. Lee and H. S. Park, "Ultra-FFS TFT-LCD with super image quality, fast response time, and strong pressure-resistant characteristics," *J. Soc. Inf. Disp.* **10**, 117-122 (2002).
- [4] I. Haller, "Thermodynamic and static properties of liquid crystals," *Prog. Solid State Chem.* **10**, 103-118 (1975).
- [5] S. T. Wu, "Birefringence dispersions of liquid crystals," *Phys. Rev. A*, **33**, 1270-1274 (1986).
- [6] W. H. De Jeu, "Physical properties of liquid crystalline materials in relation to their applications," *Mol. Cryst. Liq. Cryst.* **63**, 83-109 (1981).
- [7] S. T. Wu and C. S. Wu, "Rotational viscosity of nematic liquid crystals A critical examination of existing models," *Liq. Cryst.* **8**, 171-182 (1990).
- [8] W. Maier, A. Saupe, and Z. Naturforsch, Teil A **14**, 882 (1959). **15**, 287 (1960).
- [9] A. Lien, "Extended Jones matrix representation for the twisted nematic liquid-crystal display at oblique-incidence," *Appl. Phys. Lett.* **57**, 2767-2769 (1990).
- [10] J. W. Ryu, J. Y. Lee, H. Y. Kim, J. W. Park, G.D. Lee, and S. H. Lee, "Effect of magnitude of dielectric anisotropy of a liquid crystal on light efficiency in the fringe-field switching nematic liquid crystal cell," *Liq. Cryst.* **35**, 407-411 (2008).
- [11] H. Chen, M. Hu, F. Peng, J. Li, Z. An, and S. T. Wu, "Ultra-low viscosity liquid crystals," *Opt. Mater. Express* **5**(3), 655-660 (2015).
- [12] Y. Iwata, M. Murata, K. Tanaka, T. Ohtake, H. Yoshida, and K. Miyachi, "Novel super fast response vertical alignment-liquid crystal display with extremely wide temperature range," *J. Soc. Inf. Disp.* **10**, 1002-1019 (2014).
- [13] L. M. Blinov and V. G. Chigrinov, "Electrooptic effects in liquid crystal materials," Springer-Verlag (1994).
- [14] Y. Chen, Z. Luo, F. Peng, and S. T. Wu, "Fringe-field switching with a negative dielectric anisotropy liquid crystal," *J. Display Technol.* **9**, 74-77 (2013).
- [15] Y. Chen, F. Peng, T. Yamaguchi, X. Song, and S. T. Wu, "High performance negative dielectric anisotropy liquid crystals for display applications," *Crystals* **3**, 483-503 (2013).